

## Transport properties of superconducting amorphous W-based nanowires fabricated by focused-ion-beam-induced-deposition for applications in Nanotechnology

J. M. De Teresa<sup>1,2</sup>, A. Fernández-Pacheco<sup>1,2,3</sup>, R. Córdoba<sup>2,3</sup>, J. Sesé<sup>2,3</sup>, M. R. Ibarra<sup>1,2,3</sup>, I. Guillamón<sup>4</sup>, H. Suderow<sup>4</sup>, and S. Vieira<sup>4</sup>

<sup>1</sup>Instituto de Ciencia de Materiales de Aragón, Universidad de Zaragoza-CSIC, Facultad de Ciencias, Zaragoza, 50009, Spain

<sup>2</sup>Departamento de Física de la Materia Condensada, Universidad de Zaragoza, Facultad de Ciencias, Zaragoza, 50009, Spain

<sup>3</sup>Instituto de Nanociencia de Aragón, Universidad de Zaragoza, Zaragoza, 50009, Spain

<sup>4</sup>Laboratorio de Bajas Temperaturas, Departamento de Física de la Materia Condensada, Instituto de Ciencia de Materiales Nicolás Cabrera, Facultad de Ciencias, Universidad Autónoma de Madrid, E-28049, Madrid, Spain

### ABSTRACT

We report transport measurements of superconducting amorphous W-based nanodeposits fabricated by focused-ion-beam-induced-deposition (FIBID) technique using  $W(CO)_6$  as the gas precursor. We have found that nanowires with width down to  $\sim 100$  nm can be grown by FIBID, maintaining the relatively high  $T_C$  of  $\approx 5.2$  K shown by wider nanodeposits. The critical current found in these nanowires is in the range of  $0.8 \text{ mA}/\mu\text{m}^2$  at 2 K. At that temperature the critical field  $H_{C2}$  is found to be  $\approx 8$  T. As previously shown by STM measurements [*I. Guillamón et al., New Journal of Physics* **10**, 093005 (2008)], these nanodeposits closely follow the BCS theory and are very stable under ambient conditions. All these features pave the way for a wide range of applications of these FIBID W-based nanowires in the field of Nanotechnology.

### INTRODUCTION

The control in the growth and patterning of superconducting materials in the nanometer scale is opening interesting research fields in condensed-matter physics. Basic studies regarding one-dimensional superconductivity [1], vortex confinement [2], vortex pinning [3], etc. have been tackled recently. The fabrication of nanoSQUIDS is one of the most appealing applications of such nano-superconductors [4] as well as being supporting material for superconducting quantum bits [5].

Normally, complex nanolithography techniques such as electron-beam lithography, involving several process steps, have been used to create such superconducting nanostructures. It was recently found that a single-step technique called FIBID (Focused-Ion-Beam-Induced-Deposition) is able to produce superconducting nanodeposits with relatively high  $T_C$  up to 6 K [6-11] and closely following the BCS theory with a well-defined Abrikosov vortex lattice [10]. In the FIBID technique, a precursor gas is injected in the process chamber and by sweeping a focused ion beam (FIB) a nanodeposit is created along the path followed by the FIB. The physics and chemistry of the focused electron/ion beam deposition is complex and has been recently reviewed [12, 13]. Control in the thickness, width and length of the nanodeposits can be obtained in the nanometric range, opening vast applications in Nanotechnology.

## EXPERIMENT

The FIBID superconducting nanodeposits have been fabricated at room temperature in a commercial dual-beam equipment (Nova 200 NanoLab from FEI), which uses a 5-30 kV Ga<sup>+</sup> FIB. With a gas-injector system, the W(CO)<sub>6</sub> precursor gas is brought onto the substrate surface, where it becomes decomposed by the FIB. As previously found with XPS measurements [10], the nanodeposit composition is mainly formed by W ( $\approx 43\%$ ), C ( $\approx 40\%$ ), Ga ( $\approx 10\%$ ) and O ( $\approx 7\%$ ). TEM studies indicate that the nature of the deposit is amorphous [8], which explains the high  $T_C$  in comparison with crystalline W [14].

The nanodeposits are grown onto a previously-micropatterned SiO<sub>2</sub>//Si substrate where Al or Ti pads have been evaporated to realize contact pads for the magnetotransport measurements. We have carried out two types of deposits. The first type consists of microwires with width about 2  $\mu\text{m}$  and thickness around 1  $\mu\text{m}$ . The second type consists of nanowires with width in the range 100-250 nm and thickness in the range 100-150 nm. The aim of these experiments is first to characterize “bulk-type” W deposits in the micrometer range in order to investigate if narrow wires in the nanometer range still keep the same performance as the bulk ones.

## RESULTS

In Table I, some relevant data of the wires studied in the present work are summarized. Four microwires (M1 to M4) and four nanowires (N1-N4) have been investigated. In figure 1(a), the temperature dependence of the resistivity of the M3 microwire (grown at 20 kV/0.76 nA) is shown. It is found that  $T_C = 5.4$  K, where the critical temperature is defined at 90% of the transition ( $\rho/\rho_n=0.9$ ). From the measurements of the resistivity under several magnetic fields, the critical field,  $H_{C2}$ , has been estimated and shown in figure 1(b), being of the order of a few Tesla with a typical temperature dependence. For all the microwires (grown at different conditions as shown in Table I), the measured  $T_C$  ranges between 4.8 K and 5.4 K and seems to correlate with the room-temperature resistivity as proposed by Li et al. [11]. The values of  $T_C$  and room-temperature resistivity for all the wires (micro and nano) have been represented in figure 2a). It is generally observed that the nanowires show slightly higher resistivity than the microwires but without evident influence on the  $T_C$  value. More work is needed to understand the correlation between the room-temperature resistivity and  $T_C$ .

<i>Sample</i>	<i>V<sub>BEAM</sub> (kV)</i>	<i>I<sub>BEAM</sub> (nA)</i>	<i>Width (<math>\mu\text{m}</math>)</i>	<i>Section area (<math>\mu\text{m}^2</math>)</i>	<i>T<sub>C</sub> (K)</i>	<i><math>\rho_{300K}</math> (<math>\mu\Omega\text{cm}</math>)</i>
M1	5	1	2	1.97	5.3	163
M2	10	1.1	2	1.62	5.4	147
M3	20	0.76	2	2.10	4.7	209
M4	30	1	2	1.64	4.9	229
N1	30	0.01	0.24	0.036	5.1	309
N2	30	0.01	0.17	0.025	5.0	197
N3	30	0.01	0.11	0.016	4.8	527
N4	30	0.01	0.15	0.015	4.8	303

**Table I.** Data of the growth conditions ( $V_{BEAM}$ ,  $I_{BEAM}$ ), dimensions (width, section area), and physical properties ( $T_C$  and room-temperature resistivity) of all the wires investigated.

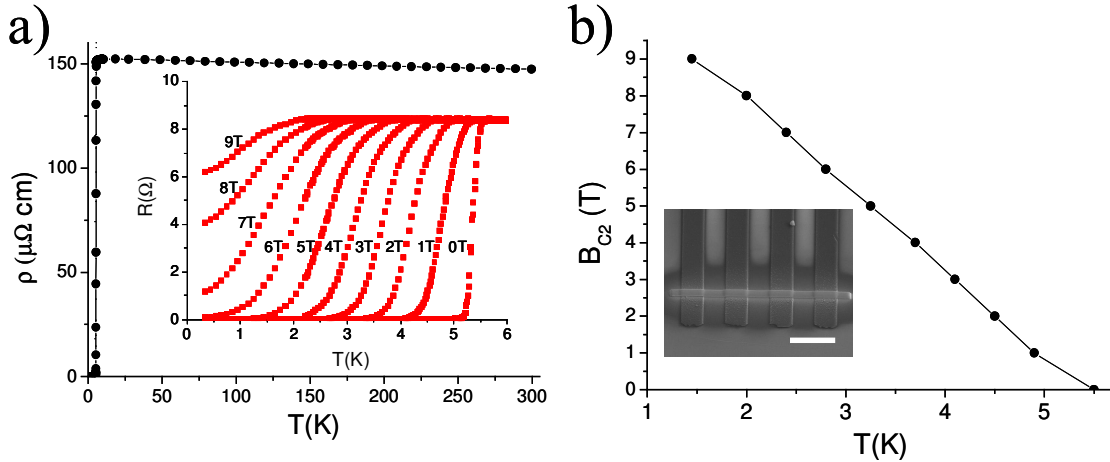


**Figure 1.** For the M3 microwire, **a)** Resistivity as a function of temperature. The inset shows measurements of the resistivity under various applied magnetic fields **b)** The critical field,  $H_{C2}$  (defined at 90% of the normal-state resistance,  $\rho/\rho_n=0.9$ ), as a function of temperature. An SEM image with the four aluminium pads used for 4-point measurements is shown in the inset, where the scale bar is  $10\ \mu\text{m}$ .

In figure 2b), the resistance-versus-temperature behaviour of one of the nanowires (N2) is shown. The nanowire resistance starts to decrease at 5.2 K and becomes zero at 4.8 K. The transition temperature ( $\approx 5\ \text{K}$ ) and transition width ( $\approx 0.4\ \text{K}$ ) are similar to those of microwires, indicating good sample stoichiometry and homogeneity. It is remarkable that a high  $T_C$  is maintained in the nanowires, which opens the route for the use of this superconducting material in nanodevices working at temperatures above liquid Helium.

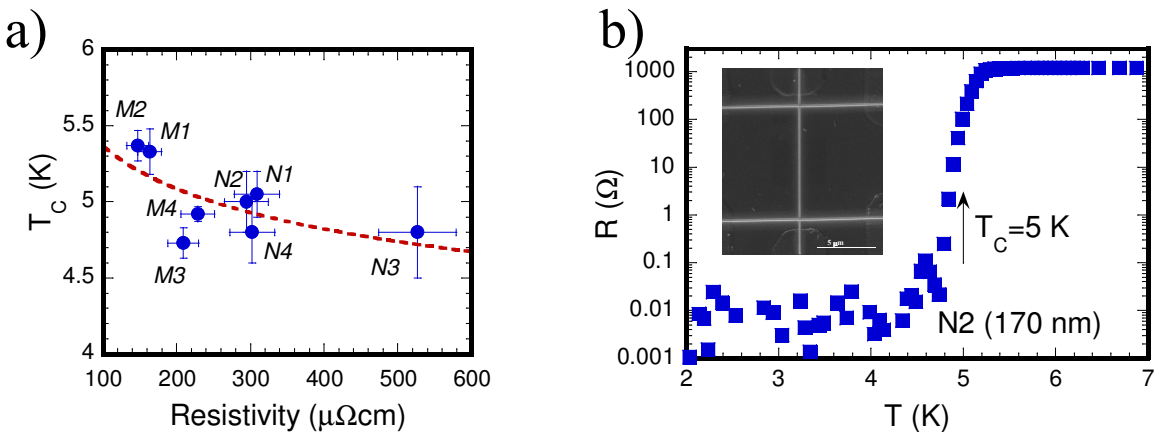


**Figure 2. a)**  $T_C$  versus resistivity of all the microwires (M1, M2, M3, M4) and nanowires (N1, N2, N3, N4) studied in the present work.  $T_C$  ranges between 4.7 and 5.4 K, with a slight tendency to decrease with the resistivity. Error bars come from the transition temperature width (y-axis) and in the determination of the wire section (x-axis). **b)** Resistance (in log scale) versus temperature of N2 (width=170 nm), indicating  $T_C=5.0\pm 0.2\ \text{K}$ . The inset is a SEM image of this nanowire (vertical line with white contrast) and the two horizontal wires for the measurement of voltage during the resistance measurements, where the current flows through the nanowire.

The resistance in the nanowires has been studied at fixed temperature as a function of the applied magnetic field with the aim of determining the range of magnetic fields where the nanowires can be used for superconducting applications. As an example of the obtained results, we focus on the behavior of the N2 sample at  $T=2$  K, represented in figure 3a). The resistance is null below  $H \sim 2$  T and increases continuously up to reaching the normal-state resistance. The value of  $H_{C2}$  is found to be  $\sim 8$  T, which is the same as found in the microwires, as shown in figure 1. All the studied nanowires show similar behavior to this as can be observed in figure 3b), where nanowires N1 to N3 are compared normalizing the resistance to the normal-state value. These results demonstrate the good translation of the superconducting properties of FIBID W deposits to the nanometric scale. A number of interesting features appearing in figure 3 will be discussed and systematically analyzed in a future focused publication. Here, we just highlight the onset of finite resistance at relatively low magnetic field, the non-linear resistance before reaching the normal-state resistance, and the dependence with the nanowire thickness of the starting magnetic field with non-zero resistance.

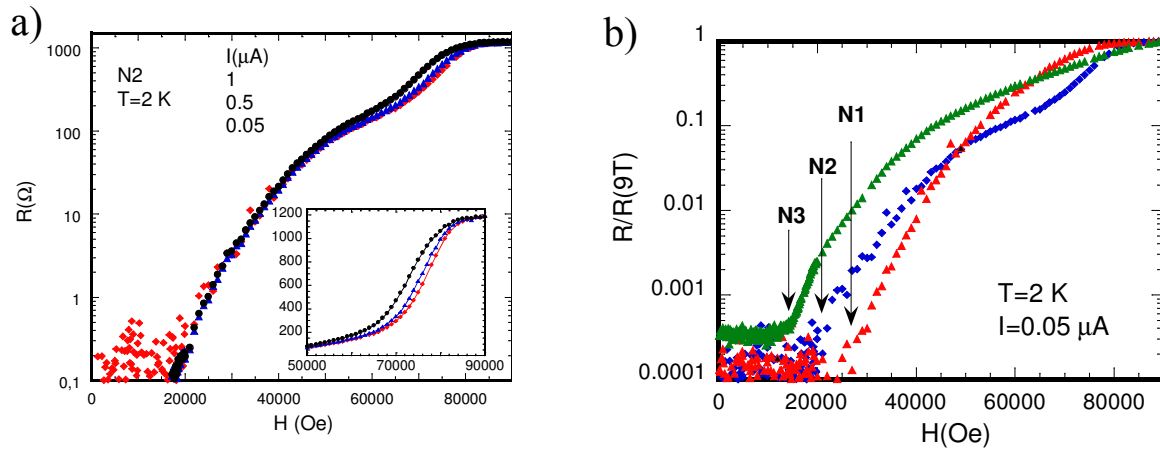


**Figure 3. a)** Resistance (in log scale) versus applied magnetic field at  $T=2$  K of N2. Three different currents have been used (1, 0.5, 0.05  $\mu\text{A}$ , shown with symbols in black, blue and red color respectively) and the inset shows in linear scale the different behavior produced by the increasing current. **b)** At  $T=2$  K, resistance normalized to the value at  $H=9$  T as a function of the magnetic field in nanowires N1, N2, and N3 using 0.05  $\mu\text{A}$  current in all cases. We would like to mention that the apparently low but finite resistance at low field in the plots is an artifact due to the limitation in the electronic equipment and should be considered equal to zero.

Another important issue to be studied in these nanowires having in mind certain applications is the value and dependence of the critical current. The results obtained on the N2 sample are shown in figure 4a) to illustrate the found dependence. At  $T=2$  K, the critical current in this nanowire is of the order of 20  $\mu\text{A}$ , decreasing for higher temperatures. Focused studies would be required to investigate if these nanodeposits show the “peak effect” of the critical current observed in other superconductors [15]. In figure 4b) we represent the resistance at  $T=2$  K normalized to the normal state as a function of the current density in several nanowires. At that temperature, the value of critical current density ranges between  $\approx 600$   $\mu\text{A}/\mu\text{m}^2$  and  $900$   $\mu\text{A}/\mu\text{m}^2$ . One could think that the dispersion in the measured values are to be ascribed to slight differences in composition, the amount of defects, error in the determination of the sectional area, etc. On

top of that, the obtained results suggest that the critical current density decreases as the nanowire width decreases (from 240 nm for N1 down to 170 nm for N2 and 110 nm for N3). This point should be addressed in more detail in future.

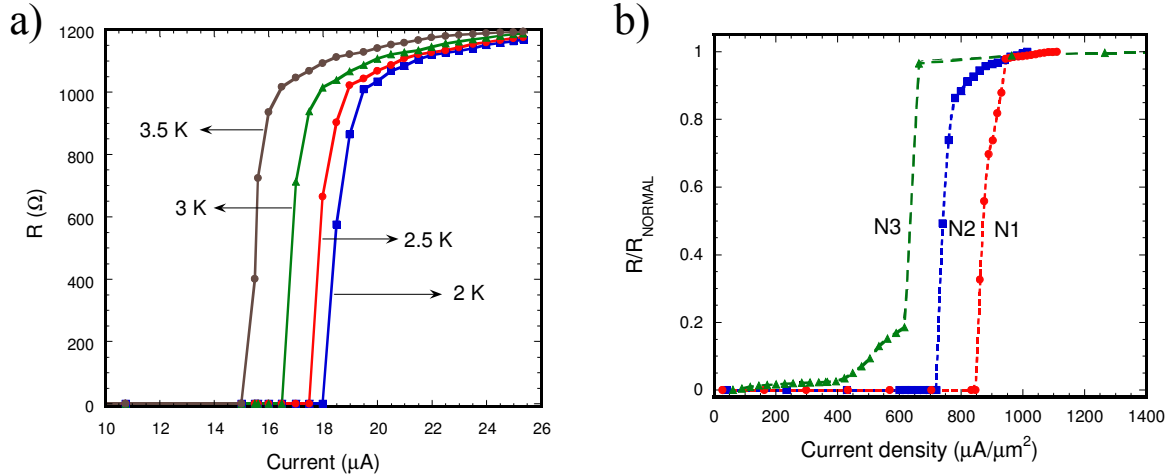


**Figure 4.** **a)** For N2 sample, resistance versus applied current at different temperatures. **b)** For several nanowires, dependence of the resistance (normalized to the value in the normal state) with the injected current density at  $T=2$  K.

## CONCLUSIONS AND OUTLOOK

In this contribution we have reported transport measurements in W-based FIBID deposits with lateral dimension ranging from  $\sim 2$   $\mu\text{m}$  down to  $\sim 100$  nm. The obtained results indicate that useful superconducting properties are retained by the narrowest wires, opening applications at the nanoscale. In particular, the values found for  $T_C$ , for the critical field  $H_{C2}$ , and for the critical current make these narrow wires promising for nanometric superconducting-based and hybrid devices. For example, mesoscopic superconductors have been proposed to be used as logic elements in quantum computing by manipulation of a controllable vortex lattice [16]. W-based FIBID nanodeposits could be feasibly used to build superconducting electronic devices due to the controllable and flexible growth at the nanometric scale and the remarkable stability and good definition of the vortex lattice. Application of these nanodeposits in the fabrication of micro/nano-SQUIDs at targeted places for high-resolution magnetometry at the nanoscale is straightforward and the first steps in that direction are being given. Fabrication of resistance-free nanocontacts for dedicated transport experiments can be also a major application of these W-based FIBID nanodeposits [7]. A long-standing problem in the electrical characterization of nanodevices is the high contact resistance of wires required to make the connection to the macroscopic world and this problem can be solved by means of superconducting wires. Moreover, fabrication of hybrid metallic-superconductor nanocontacts using these superconducting W nanodeposits seems also feasible thanks to the characteristics of FIBID W deposition. Such nanocontacts would enable the study of interesting phenomena like Andreev reflection [17] and measurements of the spin polarization of ferromagnets [18]. To sum up, the extraordinary superconducting properties of W nanodeposits performed with ion-beam-induced deposition have been highlighted and some fascinating applications anticipated.

## ACKNOWLEDGEMENTS

Financial support by Spanish Ministry of Science (through project MAT2008-06567-C02 including FEDER funding), and the Aragon Regional Government are acknowledged.

## REFERENCES

1. K.Yu. Arutyunov, D.S. Golubev, A.D. Zaikin, *Physics Reports* **464**, 1 (2008)
2. L.F. Chibotauo, A. Ceulemans, V. Bruyndoncx, and V.V. Moschalkov, *Nature* **408**, 833 (2000); I.V. Grigorieva et al., *Phys. Rev. Lett.* **92**, 237001 (2004)
3. M. Velez et al., *J. Magn. Magn. Mater.* **320**, 2547 (2008)
4. C. Granata, E. Exposito, A. Vettoliere, L. Petti, M. Russo, *Nanotechnology* **19**, 275501 (2008); C.H. Wu et al., *Nanotechnology* **19**, 315304 (2008)
5. J. Clarke and F.K. Wilhelm, *Nature* **453**, 1031 (2008)
6. E.S. Sadki, S. Ooi, K. Hirata, *Appl. Phys. Lett.* **85**, 6206 (2004)
7. A.Y. Kasumov et al., *Phys. Rev. B* **72**, 033414 (2005)
8. I.J. Luxmoore et al., *Thin Solid Films* **515**, 6791 (2007)
9. D. Spoddig et al., *Nanotechnology* **18**, 495202 (2007)
10. I. Guillamón et al., *New Journal of Physics* **10**, 093005 (2008); I. Guillamón et al., *Journal of Physics: Conference Series* (2009), *in press*
11. W. Li et al., *Journal of Appl. Physics* **104**, 093913 (2008)
12. W.F. van Dorp and C.W. Hagen, *J. Appl. Phys.* **104**, 081301 (2008)
13. I. Utke, P. Hoffmann, J. Melngailis, *J. Vac. Sci. Technol. B* **26**, 1197 (2008)
14. M.M. Collver and R.H. Hammond, *Phys. Rev. Lett.* **30**, 92 (1973)
15. M.C. Hellerqvist et al., *Phys. Rev. Lett.* **76**, 4022 (1996); N. Kokubo et al., *Phys. Rev. Lett.* **75**, 184512 (2007)
16. Dorsey A.T., *Nature* **408**, 783 (2000)
17. A. Shailos et al., *Europhysics Letters* **79**, 57008 (2007)
18. J.R. Soulen et al., *Science* **282**, 85 (1998)